An anatomical aortic root model based on N-sided patches for elastic simulation

Tamás Umenhoffer[1]

[1] Department of Control Engineering and Informatics, Budapest University of Technology and Economics, Budapest, Hungary

Abstract

In this paper we describe our framework of aortic root simulation for valve sparing aortic root replacement surgery, and examine how N-sided patches can be used to increase the accuracy of our anatomic model. As modeling with N-sided patches gives more freedom to the user than traditional four-sided patches, the definition of our aortic root geometry model is more directly bound to anatomical features. Moreover, the triangular geometry after tessellation gives more even triangle distributions as in case of traditional patches, thus can make elastic simulation more robust.

1. Introduction
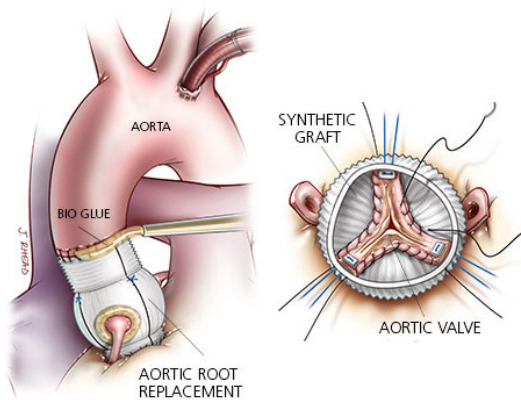
Figure 1: *Valve sparing aortic root surgery* [†].

Aortic root surgery is necessary if a disease has developed that affects the portion of the aorta closest to the heart: the aortic root. The most common diseases are high blood pressure and Marfan syndrome (when the connective tissues are weakened due to abnormal production of fibrillin), which causes aortic root enlargement or aortic root aneurysm. In case of these diseases the aortic valve is not diseased, unlike in case of aortic valve stenosis, when the valves are too narrow and stiff.

If the valves are not diseased valve sparing aortic root re-placement can be used. During these operations the patient's aortic root with valves are removed and replaced with a synthetic tube called graft. However the patient's own valves are preserved and sewed back into the inside of the graft. The coronary arteries are also attached. This operation, unlike using synthetic valves, avoids the use of life-long blood thinners, thus recommended for active and young patients. The graft is highly durable and does not require any additional medicines, while the patients own valves potentially will last the rest of their lives.

Figure 1 shows the aortic root after valve sparing aortic root surgery and the inner side of the graft after the valves are sewed in. On the left side we can see a black line running on the outer side of the graft. This has special meaning, it shows where the comissures of the valves should be sewed in. These lines are drawn on the grafts by the producer of the graft and the three lines have even angle distribution on the circle of the tube. However, patients have their own specific comissure angle distributions, which is usually not considered by the surgeon and the valves are sewed in the predefined even distributions. This is because the measurement of patient specific angles are not straightforward during he operation, but recently special tools have been developed that make this measurement accurate and fast, thus en-

---

[†] Image courtesy of Intermountain Medical Center Heart Institute (https://intermountainhealthcare.org/services/heart-care/treatment-and-detection-methods/aortic-root-replacement/)
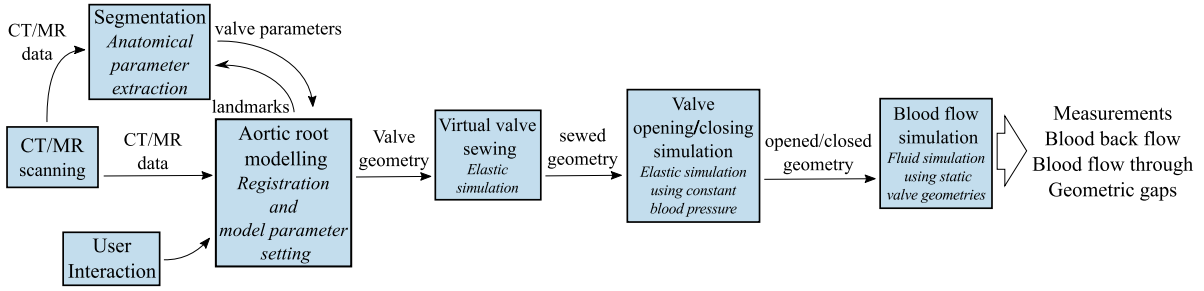
Figure 2: *The main workflow of our framework.*
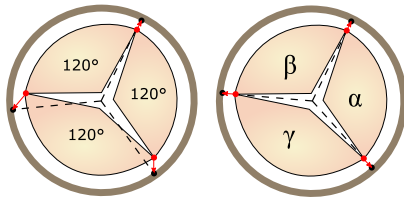
Figure 3: *Valve sewing methods with even and with patient specific leaflet angle distributions.*

ables the sewing using the patient specific distributions. Yet no database exists that would show the physiological benefit of the more advanced surgery technique, though it probably has. Figure 3 shows the difference between the two valve sewing methods.

Our goal is to try to prove the benefits using computer simulations [8]. We defined a framework to create patient specific geometric models of the aortic root and the valves and simulate valve opening and closing and blood flow in case of both surgery techniques. We believe that measuring the blood back flow and flow through or the geometric gaps between valve leaflets will provide us the necessary information.

To run the simulations we needed to define an aortic root geometry based on anatomical features. This paper compares two approaches for the geometric definition of the aortic root: four-sided patch models and N-sided patch models. We compare the two techniques regarding how they describe the underlying anatomical surface, and their effectiveness during elastic simulation.

2. Simulation workflow

The main workflow of our system is shown on Figure 2. As we need patient specific aortic root models we use medical imaging data, particularly CT or MR scans. These scans serve only as a base for the modeling procedure, which is not fully automated, it needs significant professional user inter-

action. If the geometric model is ready we can run our simulations.

In most aortic root simulation systems a coupled elastic and fluid simulation is used. It means that elastic and fluid simulation steps are run alternately and iteratively to take both phenomena into account. The main drawback of this technique is that data conversion is usually needed when changing to one solver to an other. We avoid this problem with making simplifications applicable specifically for the aortic valve surgery problem.

Our final measurements that show the effectiveness of a surgery technique would be the amount of blood that flows through the aortic root when the valves are in opened position. Similarly the amount of blood that can flow back if the valves are closed is also a very important value. We can also measure geometric gaps between the valve leaflets in closed position. These measurements does not require coupled elastic-fluid simulations, only fluid simulation with a static geometry (the opened or closed leaflets).

As the fully opened and closed state of the valves take only a short period of one hearth cycle, when the blood pressure in the aorta is defined by the maximal ventricular pressure, no fluid simulation is needed to calculate the opened and closed valve shapes, only elastic simulation. During these elastic simulations blood pressure is modeled with a constant force. Virtual sewing of the aortic valves should also be simulated with the purely elastic model.

As we are interested in the valve functioning after surgery, the exact patient specific aortic root model is not used during simulation, only the models of the valves. The grafts has a simple tube shape which can be modeled analytically in contrast to the more complex shapes of the sinuses of Valsava (see Figure 4). On the other hand we also created the geometric model of the sinuses of Valsalva, which provides a useful visual feedback during medical data registration, and this model can also be used in the future to simulate the patients own aortic root before surgery.
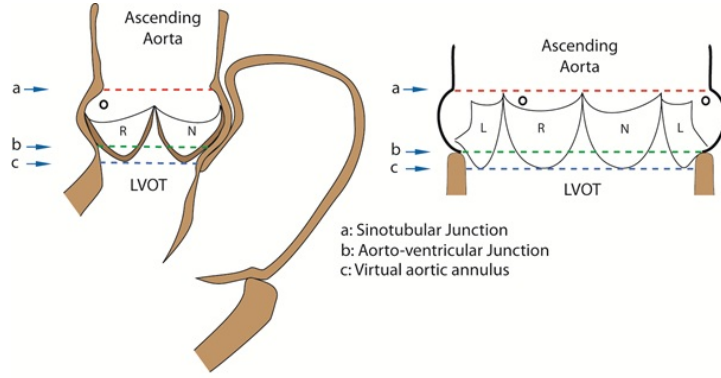
Figure 4: *The anatomy of the aortic root and aortic valves.*

Name	Type	Default Values	Description
commissure1	3D vector	(0, 17.5, 13.44)mm	Common suspension point of the L and N valves.
commissure2	3D vector	(11.64, 17.5, -6.72)mm	Common suspension point of the R and N valves.
commissure3	3D vector	(-11.64, 17.5, -6.72)mm	Common suspension point of the L and R valves.
leafletTipPoint	3D vector	(0, 15.03, 0)mm	Valve intersection point.
annulusRadius	float	11.58 mm	The radius of the annulus
valsalvaRadius	float	14 mm	The largest radius of the aortic root
valsalvaMaxRadiusHeight	float	0.25	Position of maximal radius on aortic root axis (0-1)
ostiumR	3D vector	(0, 14, -14.2) mm	Base point of right coronal ostium
ostiumL	3D vector	(-12.2, 14, 7) mm	Base point of left coronal ostium
valsalvaSlope	float	0.05	Slope of the sinuses of Valsalva
valsalvaCurvature	float	3	Curvature of the sinuses of Valsalva

Table 1: *Aortic root modeling parameters.*

3. Aortic root model

Our aortic root model is constructed by spline surfaces, where spline control points are controlled by anatomical features. Many articles can be found that deals with aortic valve anatomy [4], but for us the work of Calleja et al. [1] proved to be the most useful. Here we could find various anatomic measurements and average values of the aortic root.

The aortic valves are located in the lower thickened part of the ascending aorta called aortic root. Each valve has its own cavity called the sinus of Valsalva. The roughly circle shaped section where the aortic root and the left ventricle connects is called annulus, which is signed with c on Figure 4. The center and radius of this circle can be well identified on CT and even on lower resolution MRI data so these will be our first model parameters.

Note that in our model the aortic root defines our coordinate system where the xz plane is at the annulus and y points in the direction of the ascending aorta.

The round shaped connection between the aortic root and the ascending aorta is called sinotubular junction (STJ) (la-bel a on Figure 4). The topmost suspending points of the aortic valves (commissures) are located at this level. These commissure can be well identified on medical data, and they also define the center and radius of the STJ. The commissures are not placed evenly on the circle of the STJ, their angles are patient specific and will play a dominant role in our simulations.

Aortic valves are little pockets with sharp edges at the top, which join in a single point when the valves are closed. This point can also be identified from CT data. We placed the lowest points of the valves symmetrically between two commissures at the level of the annulus.

If the above parameters are given, the valves can be constructed, but we need some extra parameters for the sinus of Valsalva. The largest radius of the aortic root and its position along the y axis should also be given. We also introduced parameters to control the curvature and slope of sinuses.

The final modeling parameter set is listed in table 1 with their type, default values and brief description.

4. Four-sided patch based geometry

As the aortic root is a smooth, rounded surface, thus a smooth geometric representation should be used. Spline based surfaces are such representations, and they are widely used in computer aided design. The traditional approach is to divide the surface into a set of smaller, four-sided patches. The four sides of these patches are four splines and the internal points are interpolated from the edge splines. Four sided patches enable simple parameterization which makes interpolation and tessellation simple and effective.

The top row of Figure 5 shows the aortic root surface defined by four-sided patches. The green lines show the splines that define the patches, and blue cubes indicate spline control points. We can see that the sinuses of Valsalva can described quite well with these patches. However the valve leaflets are hard to describe with four-sided domains as shown on the rightmost image. Our solution was to collapse the lowest row of control points to a single point. In practice they are not on the same location, only close enough, as fully merging them would result in zero area triangles after tessellation, which would ruin physical simulation.

The effect of shrunk bottom splines can be clearly seen on Figure 6, where the top row shows the tessellated geometry of the four-sided patch based model. Here we used quad polygons, but the final simulation will be run on triangles. The rightmost image shows the tessellated valve, which shows shrinking triangle areas as we get close to the bottom of the leaflet. An other drawback of this model is that the leaflets and the Valsalva don't share a common spline at their intersections. This means that we cannot ensure that the edges of the leaflets and the Valsalve surface connect without gaps or collisions.

5. N-sided patch based geometry

The limitations of four-sided patches led us to try N-sided patches for geometry definitions. We used the Sketches system (ShapEx Ltd. Budapest) which is CAD system using a curvenet-based design scheme. The process begins with creating a curve network representing the boundaries and feature lines of the object, then the interpolating surfaces are expected to be automatically generated over the curve network. Transfinite surfaces are particularly suitable for this approach, since they are determined solely by boundary curves and cross-derivatives. For additional information about transfinite surface interpolation the reader should refer to the work of Várady et al. [9]. About generalized Coons patches, which were used in our model the reader should refer to a paper [7] from the same authors.

The bottom row of Figure 5 shows our N-sided patch model. We can see that the boundary curve network is strictly defined by the anatomical parameters, like commissure positions, the arc of the sinuses, the arc of the annulus and the STJ. With this modeling approach the sinuses can be enhanced. The crown shape between the annulus and the sinuses is often referred by anatomic descriptions about the aortic root, and can hardly be modeled with four-sided patches. On the other hand N-sided patches could handle it without injecting any additional control points and patches.

The differences are even bigger in case of the valve leaflets. Using two triangular patches the leaflet can be modeled without collapsing geometry. As the Valsalva model and the valve models share common boundary curves, their intersections are perfect. The tessellated geometry of the N-sided patch model can be seen on the bottom row of Figure 6. The tessellation does not seems as structural as in case of traditional patches, as it lost its grid structure. We can also clearly see regions with different triangular densities. On the other hand the the leaflet geometry (rightmost image) shows even triangle distributions. In the following section we examine, how these two models compare in our elastic simulations.

6. Simulation tests

We used a finite element [2] elastic simulation with triangular prism elements. The first step of our workflow is to simulate the sewing of the leaflets to the walls of the synthetic graft. We compared the two patch models during this simulation. The valves were stretched to a graft with greater radius than the patients own aortic root radius.

Finite element simulations perform better if the elements have roughly the same size. Too small element sizes should also be avoided as it results in numerical errors due to insufficient floating point precision. Our first measure was to calculate the triangle areas in case of both patch models. On the left side of Figure 7 the four-sided patch model can be seen, and on the right the tessellated N-sided patch model. The triangle areas are color codes such that red areas show small triangles and blue areas show large triangles. The traditional patch model shows small triangles at the bottom of the leaflet, and large triangles at the top. The N-sided patch model has much more even triangle area distribution, a few smaller triangle appears at the tip of the leaflet, and triangles around the edges are slightly larger.

We compared several leaflet stretching simulations with the two models. Our system is an explicit finite element method which was successfully used in elastic simulations [3]. Unfortunately it has a drawback that small time steps should be used to avoid the explosion of the simulation and to achieve correct results. We also have to introduce a velocity damping and let the simulation slowly converge to maintain stability. To achieve best computing performance the time step should be set as high as possible, while the damping should be set at its lowest possible level.

We run the stretching test with different damping and time step values for both patch models. We let the simulation run to simulate two seconds of motion. We used material parameters that correspond to human aortic valve tissue: 1MPa
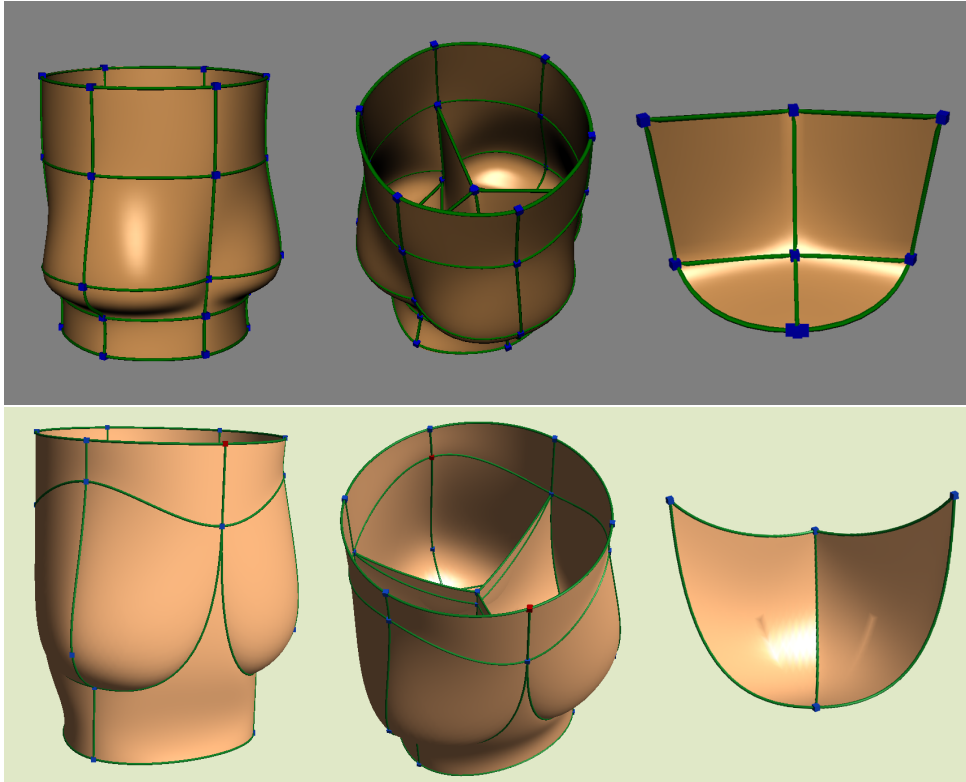
Figure 5: *Four-sided (top) and N-sided (bottom) patch models of the aortic root and the valve leaflets (right).*
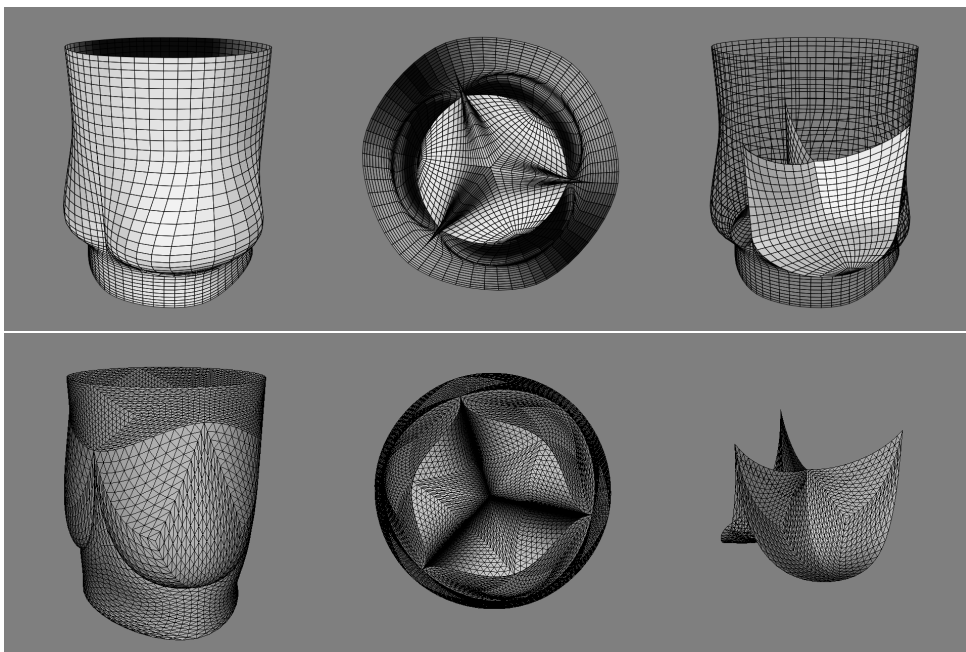
Figure 6: *Tessellation of the four-sided (top) and N-sided (bottom) patch models.*
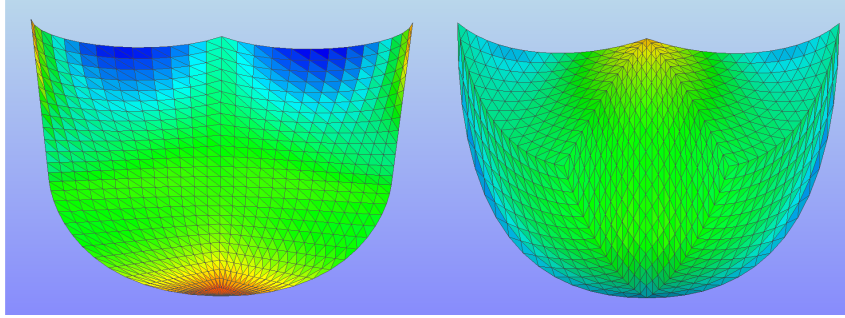
Figure 7: *Color coded triangle areas of the four-sided (left) and N-sided (right) patch models. Red colors mean smaller, blue colors mean larger triangles.*

Young modulus [6, 5], 0.3 Poisson ratio, 0.6 mm leaflet thickness [10]. Table 2 shows the results. The table entries shows the time interval in seconds the simulation could calculate without exploding. If this time value reached 2 seconds, the simulation was stable, otherwise it was terminated. The table shows that the N-sided patch model could simulate time steps of 0.005 seconds with all our damping factors, while four-sided patches could achieve this only with the smallest time step. The N-sided patch model could even run the 0.01 second time step with the highest damping factor.

Some results are also shown on Figure 8. The blue geometry shows the N-patch valve model, while the yellow shows the four-sided. The two geometries are drawn on top of each other on the right. The valves are shown from above. The top row shows simulations with the smallest time step with 0.2 damping, where both model succeeded. The results are also close to each other: both models have similar gaps between the leaflets after stretching. The bottom row shows a simulation with higher time step. The N-patches model could calculate the full stretching, while the four-sided model went unstable and stopped the simulation in an early stage, and the valves could only slightly open.

7. Conclusion and future work

We found that N-sided patches can be successfully used for the definition of an anatomically based aortic root models. It has several advantages over traditional four-sided patches regarding even triangle area distributions, and can better define the complex shape of the sinuses and the leaflets. We shown that it the triangular topology N-sided patches provide more robust elastic simulations, which enables us to use higher time step values.

As a future work we would like to test the new model for the opening and closing simulations of the valves. We already have successful simulation tests with the four-sided geometry and we expect the N-sided model to perform better. We also would like to refine our curve boundary for the N-sided model to better describe some anatomical features we still could not include in either of our models, and would like to decrease the tessellation differences in various areas of the sinuses of Valsalva.

Acknowledgements

References

		Damping			
dt(s)		0.3	0.25	0.2	0.15
0.001	4-sided	**2s**	**2s**	**2s**	**2s**
	N-patch	**2s**	**2s**	**2s**	**2s**
0.005	4-sided	0.1s	0.095s	0.08s	0.065s
	N-patch	**2s**	**2s**	**2s**	**2s**
0.01	4-sided	0	0	0	0
	N-patch	**2s**	1.82s	1.445s	1.09s
0.05	4-sided	0	0	0	0
	N-patch	0	0	0	0

Table 2: *Aortic root modeling parameters.*

1. Calleja A., Thavendiranathan P., Ionasec R.I., et al. Automated quantitative 3-dimensional modeling of the aortic valve and root by 3-dimensional transesophageal echocardiography in normals, aortic regurgitation, and aortic stenosis: comparison to computed tomography in normals and clinical implications. In *Circ Cardiovasc Imaging*, pages 99–108, 2013.

2. K.J. Bathe. *Finite Element Procedures in Engineering Analysis*. Prentice-Hall civil engineering and engineering mechanics series. Prentice-Hall, 1982.

3. Gilles Debunne, Mathieu Desbrun, Marie-Paule Cani,
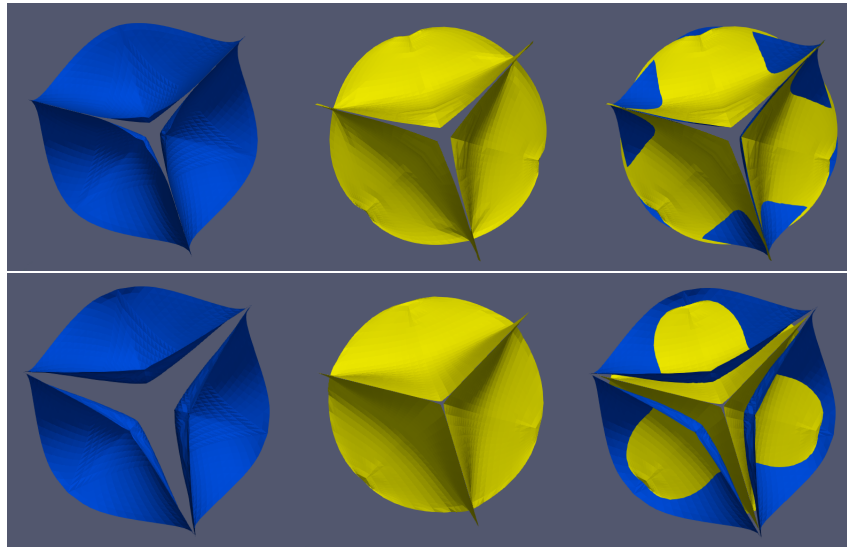
Figure 8: *Simulation results using the N-sided (left) and the four-sided (middle) models. The top row uses a smaller time step, where both models succeeded with similar results (left). The bottom row uses a larger time step where the four-sided model resulted unstable simulation and was aborted.*

and Alan H. Barr. Dynamic real-time deformations using space & time adaptive sampling. In *Proceedings of the 28th Annual Conference on Computer Graphics and Interactive Techniques*, SIGGRAPH '01, pages 31–36, New York, NY, USA, 2001. ACM.

4. Charitos Efstratios I. and Sievers Hans-Hinrich. Anatomy of the aortic root: implications for valve-sparing surgery. In *Annals of Cardiothoracic Surgery*, volume 2, 2013.

5. M S Hamid, H N Sabbah, and P D Stein. Vibrational analysis of bioprosthetic heart valve leaflets using numerical models: effects of leaflet stiffening, calcification, and perforation. *Circulation Research*, 61(5):687–694, 1987.

6. A. Hasan, K. Ragaert, Wojciech Swieszkowski, S. Selimovic, A. Paul, G. Camci-Unal, R. Mohammad, M.R. Mofrad, and Ali Khademhosseini. Biomechanical properties of native and tissue engineered heart valve constructs. *Journal of Biomechanics*, 47(9):1949–1963, 2014.

7. Péter Salvi, Tamás Várady, and Alyn Rockwood. Ribbon-based transfinite surfaces. *Computer Aided Geometric Design*, 31(9):613 – 630, 2014.

8. László Szirmay-Kalos, György. Antal, and Ferenc Csonka. *Háromdimenziós grafika, animáció és játékfejlesztés*. ComputerBooks, Budapest, 2003.

9. Tamás Várady, Alyn P. Rockwood, and Péter Salvi. Transfinite surface interpolation over irregular n-sided domains. *Computer-Aided Design*, 43(11):1330–1340, 2011.

10. K.L. Weind, C.G. Ellis, and D.R. Boughner. Aortic valve cusp vessel density: Relationship with tissue thickness. *The Journal of Thoracic and Cardiovascular Surgery*, 123(2):333 – 340, 2002.